Ilam University of Medical Sciences

Plant Biotechnology Persa

Online ISSN: 2676-7414

Homepage: https://pbp.medilam.ac.ir

Biotechnological and Pharmacological Perspectives on Plant-Produced PD-L1-Targeting Single-Domain Antibodies (VHHs/Nanobodies)

Maryam Behyari [1]✉, **Mahla Behyari**[2]

[1] Department of Cancer Cell and Molecular Biology, University of Leicester, Leicester, UK
[2] Department of Tissue Engineering, Tehran University of Medical Sciences, Tehran, Iran

Article Info

Article type:
Review Article

Article History:
Received: 29 July 2026
Revised: 03 Sep 2026
Accepted: 05 Sep 2026
Published Online:

✉ ***Correspondence to:***
Maryam Behyari

Email:
maryam.behyary@gmail.com

A B S T R A C T

Objective: Immune checkpoint inhibitors targeting the PD-1/PD-L1 axis have transformed cancer therapy, but conventional mAbs are limited by poor tumor penetration, prolonged systemic exposure, irAEs, and high production costs. VHHs and plant molecular farming may address these limitations, yet their integration remains largely unexplored. This scoping review summarizes evidence on PD-L1 inhibition by VHHs, plant-based VHH production, ICI efficacy and safety in NSCLC, and VHH pharmacokinetics.

Methods: Peer-reviewed studies published from 2012 to 2025 were identified through PubMed/MEDLINE, Web of Science, PDB, and ClinicalTrials.gov. Eligible studies addressed PD-L1 structure, VHH engineering and production, plant-based expression, ICI outcomes in NSCLC, or nanobody pharmacokinetics. Data were systematically extracted, and methodological quality was assessed using RoB 2, ROBINS-I, and AMSTAR 2 according to study design.

Results: From 1,247 records identified, 149 full-text articles were assessed, and 62 studies were included. Structural analysis identified key PD-L1 hotspots (F19, Y56, R113, M115). The KN035 nanobody (PDB: 5JDS) competes with PD-1 for the same surface on PD-L1 through a 21-amino-acid loop with approximately 1,000-fold stronger binding than PD-1. VHHs (~15 kDa) have short half-lives (hours) due to renal filtration. Plant expression of VHH-Fc fusions in Nicotiana benthamiana has been reported at yields up to 110.90 ± 6.46 mg/kg fresh weight, depending on subcellular targeting and protein engineering. No plant-produced anti-PD-L1 VHH has been reported to date. Clinical data show that ICI combination regimens achieve HR OS as low as 0.56 (95% CI 0.45–0.70) in the updated analysis of KEYNOTE-189, with Grade ≥3 immune-mediated adverse event rates of approximately 8–11% across ICI combination trials. No human clinical trial data exist for VHHs in NSCLC.

Conclusions: Plant-produced VHHs represent a promising but currently unproven approach for PD-L1 inhibition. The structural and pharmacological rationale is strong, but clinical and biotechnological evidence is lacking. Phase I/II trials and proof-of-concept plant expression studies are warranted.

Keywords: PD-L1, VHH, Nanobody, Plant Molecular Farming, Plant Proteins

➢ **How to cite this paper**
Behyari M, Behyari M. Biotechnological and pharmacological perspectives on plant-produced PD-L1-targeting single-domain antibodies (VHHs/nanobodies). Plant Biotechnology Persa. 2026; 8(4): Proof.

© The Author(s)
CC BY NC

Introduction

Programmed cell death protein 1 (PD-1, CD279) is an inhibitory receptor expressed on the surface of activated T lymphocytes, B cells, and myeloid cells. Its primary ligands, PD-L1 (B7-H1, CD274) and PD-L2 (B7-DC, CD273), are type I transmembrane glycoproteins that belong to the B7 family of immune regulatory molecules. Under physiological conditions, the PD-1/PD-L1 interaction serves as a critical checkpoint for maintaining peripheral immune tolerance and preventing autoimmunity by limiting excessive T-cell activation and tissue damage during inflammatory responses [1,2].

The molecular mechanism of PD-1-mediated immunosuppression involves the recruitment of SRC homology region 2 domain-containing phosphatases 1 and 2 (SHP-1 and SHP-2) to the immunoreceptor tyrosine-based inhibitory motif (ITIM) within the intracellular domain of PD-1. This recruitment initiates a signaling cascade that dephosphorylates key components of the T-cell receptor (TCR) signaling pathway, including CD3ζ and ZAP-70, leading to inhibition of T-lymphocyte proliferation, cytokine production, and cytotoxic effector function [3]. Prolonged PD-1 engagement ultimately drives T-cell exhaustion, a state characterized by progressive loss of effector function, metabolic dysregulation, and eventual apoptosis of tumor-specific T cells [3].

The clinical relevance of this pathway is underscored by the observation that PD-L1 is overexpressed across a wide spectrum of human malignancies, including melanoma, NSCLC, breast cancer, colorectal cancer, and hepatocellular carcinoma [4,5]. Tumor cells exploit this pathway by upregulating PD-L1 expression on their surface, effectively co-opting an intrinsic self-tolerance mechanism to evade immune surveillance and destruction by cytotoxic T lymphocytes [6,7]. This immune evasion strategy represents a fundamental hallmark of cancer and has emerged as a primary target for therapeutic intervention.

The therapeutic blockade of the PD-1/PD-L1 axis with monoclonal antibodies (mAbs) has fundamentally transformed the landscape of cancer treatment over the past decade. Full-length mAbs such as pembrolizumab, nivolumab, atezolizumab, and durvalumab have demonstrated remarkable clinical efficacy across multiple tumor types, with particularly impressive results in NSCLC, which represents approximately 85% of all lung cancer diagnoses and remains the leading cause of cancer-related mortality worldwide [8].

In NSCLC, PD-1/PD-L1 inhibitors have revolutionized systemic treatment paradigms. Pembrolizumab monotherapy demonstrated superior overall survival compared to chemotherapy in patients with PD-L1 tumor proportion scores (TPS) ≥50% in the KEYNOTE-024 trial (HR OS 0.63, 95% CI 0.47–0.86) and in patients with TPS ≥1% in the KEYNOTE-042 trial (HR OS 0.81, 95% CI 0.71–0.93) [9,10]. Combination regimens of ICIs with platinum-based chemotherapy have further improved outcomes, with KEYNOTE-189 demonstrating an HR OS of 0.49 (95% CI 0.38–0.64) in the initial analysis for non-squamous NSCLC, and KEYNOTE-407 showing an HR OS of 0.64 (95% CI 0.49–0.85) in squamous NSCLC [11,12]. In the updated analysis of KEYNOTE-189, the HR OS was 0.56 (95% CI 0.45–0.70) [13]. Network meta-analyses have confirmed that ICI-based combination regimens consistently achieve superior survival outcomes compared to chemotherapy alone [21,22,23].

Despite these successes, the efficacy of mAb-based ICIs is fundamentally limited by inherent pharmacological and immunological challenges. The most prominent limitation is the large molecular size of mAbs (approximately 150 kDa), which severely restricts their efficient and deep penetration into the dense extracellular matrix (ECM) of solid tumor masses [17]. This penetration defect is particularly evident in tumors with dense histology, such as squamous NSCLC, where high ECM density and elevated intratissue pressure impair the uniform diffusion of large molecules [18]. Poor and heterogeneous penetration leads to low effective drug concentrations in the tumor core and survival of tumor cells in areas of high hypoxia, contributing to therapeutic resistance.

A second major limitation is the prolonged half-life of mAbs, which is mediated by their interaction with the neonatal Fc receptor (FcRn). This interaction protects mAbs from lysosomal degradation and recycles them back into circulation, extending their half-life to 2–4 weeks [17]. While this extended half-life offers the convenience of infrequent dosing, it also results in prolonged systemic drug accumulation in healthy organs and tissues. This systemic accumulation is directly associated with an increased risk of immune-related adverse events (irAEs), including psoriasis, cystitis, colitis, pneumonitis, and thyroid dysfunction [19,20]. Clinical reports have clearly documented that serious irAEs can occur after treatment with ICIs, and network meta-analyses have confirmed that the highest survival advantage achieved with aggressive combination regimens comes at the cost of the highest rates of Grade ≥3 immune-mediated adverse events [21,22].

A third limitation is the inefficacy of mAb-based ICIs in certain patient subgroups, particularly those with low or absent PD-L1 expression. While PD-L1 expression is a useful predictive biomarker, a substantial proportion of patients with PD-L1-negative tumors still derive limited benefit from ICI monotherapy, and combination strategies are often required [21]. Furthermore, emerging mechanisms of therapeutic resistance, including compensatory pathway activation (e.g., PD-L1/CD80 interaction) and post-translational modifications of PD-L1 (e.g., glycosylation), further limit the efficacy of conventional mAbs [4,54,55].

Finally, the high manufacturing costs and complex cold-chain logistics associated with mAb production in mammalian cell culture systems pose significant barriers to global accessibility, particularly in resource-limited settings [24].

These challenges have created an urgent need to design next-generation inhibitory agents with improved molecular properties. Single-domain antibodies (VHH/nanobodies), derived from camelid heavy-chain antibodies, have emerged as a promising alternative platform for PD-L1 inhibition [25]. VHHs represent the smallest naturally occurring antigen-binding fragments, with a molecular weight of approximately 15 kDa, and possess several structural features that distinguish them from conventional antibody fragments [26].

The VHH scaffold consists of a single immunoglobulin variable domain that naturally lacks the light chain, resulting in a compact and highly stable structure [25]. This architecture confers several critical advantages. First, VHHs exhibit high thermal stability, with melting temperatures often exceeding 70°C, simplifying manufacturing, formulation, and storage processes [25]. Second, the extended CDR3 loop of VHHs, which is typically longer than that of conventional antibodies, allows targeting of cryptic or focal epitopes that are inaccessible to full-length mAbs [26]. Third, the small size of VHHs enables superior tissue penetration and homogeneous distribution throughout tumor masses, potentially achieving higher effective drug concentrations at the site of action [27].

Recent structural studies have demonstrated that VHHs can achieve sub-nanomolar binding affinity to PD-L1 and may inhibit the PD-1/PD-L1 interaction through multiple mechanisms. The KN035 nanobody competes with PD-1 for the same flat surface on PD-L1 through a single 21-amino-acid loop that forms two short helices and develops key hydrophobic and ionic interactions with PD-L1 residues such as Ile54, Tyr56, and Arg113 [28]. A diverse panel of 16 novel VHHs specific to PD-L1 has been characterized, demonstrating affinities ranging from 0.7 nM to 5.1 μM and the ability to completely inhibit PD-1 binding to PD-L1 [29]. Importantly, CD80 and PD-1 share a highly overlapping binding site on PD-L1, and a panel of VHHs has been identified that is expected to inhibit CD80 binding, suggesting that dual PD-1/CD80 blockade may be achievable [29,30].

The pharmacokinetic properties of VHHs are equally critical to their therapeutic potential. Due to the lack of an Fc domain, unengineered VHHs bypass FcRn recycling and are rapidly cleared by renal glomerular filtration, with a half-life in hours [17]. While this short half-life reduces systemic exposure and may lower the risk of irAEs, it also requires half-life extension strategies for therapeutic applications. Several engineering

approaches have been developed to address this limitation, including Fc fusion (e.g., envafolimab, half-life ~23 days), albumin-binding domain fusion, and PEGylation [31,32].

A critical but often overlooked dimension in the development of next-generation biopharmaceuticals is the production platform. Conventional manufacturing of therapeutic antibodies relies on mammalian cell culture systems, particularly Chinese hamster ovary (CHO) cells, which require expensive bioreactors, complex media, and stringent cold-chain logistics. Plant molecular farming—the use of plants as bioreactors for recombinant protein production—offers a compelling alternative [33,34].

Plant-based pharmaceutical production systems offer notable economic and practical advantages over traditional fermentation and cell culture methods. The establishment of a molecular farming facility generally requires 50–80% less capital investment than a mammalian cell culture plant, and per-unit production costs can be as low as 1–10% of those in conventional systems [35]. As plants can be cultivated on a large scale agriculturally, production is highly scalable, increasing output simply by expanding planted acreage, which yields economies of scale and significantly lowers the cost per dose at high volumes [35].

Plant expression systems also inherently eliminate the risk of contamination by human or animal pathogens that can plague animal cell cultures, since most human pathogens cannot replicate in plants [33]. This safety barrier reduces the burden of stringent aseptic processing and the containment measures required during manufacturing. Furthermore, certain plants used in molecular farming have remarkably fast growth and can rapidly produce target proteins. Nicotiana benthamiana, in particular, can complete a growth cycle in as little as 4–5 weeks and is amenable to rapid transient expression technologies, allowing the production of vaccine or antibody candidates in days or weeks [36].

Advances in glycoengineering have largely overcome historical concerns about plant-specific glycosylation, enabling plants to add human-compatible sugar moieties to recombinant proteins [37]. Modern transgenic plants can carry out complex post-translational modifications, proper protein folding, and assemble multimeric proteins like mammalian cells [38]. Additionally, specific seed-based plant systems (e.g., rice) naturally compartmentalize and stabilize proteins in dry seeds, obviating cold-chain storage requirements and preserving pharmaceutical proteins for long periods at ambient temperatures [39].

VHHs are ideally suited for plant-based expression for several reasons. First, their small size and simple structure reduce the metabolic burden on the plant cell, allowing for high-level accumulation [40]. Second, VHHs are naturally stable and can fold correctly in the plant cellular environment [41]. Third, VHHs do not require complex glycosylation for activity, eliminating concerns about plant-specific glycan structures that can be immunogenic in humans [40,41]. Finally, the high thermal stability of VHHs simplifies downstream processing and storage [25].

Transient expression in N. benthamiana has been widely used for VHH production, with yields at the mg/kg level for some VHH-Fc fusions [41,43]. Plant-produced anti-HER2 VHH-FcK antibodies have demonstrated binding to HER2-positive breast cancer cells, inhibition of cell migration, and superior antitumor activity in immune-deficient mice [44]. Plant-produced VHHs targeting EGFR and HER2 displayed on potato virus X nanoparticles increased retention time and myeloid cell recruitment in the tumor microenvironment in HER2+ mouse tumor models [45].

Although anti-PD-L1 monoclonal antibodies such as atezolizumab and pembrolizumab have been successfully expressed in *Nicotiana benthamiana*, they remain full-length mAbs and therefore retain the pharmacokinetic limitations associated with conventional antibody therapeutics [42]. The integration of VHHs' compact structure, tissue penetration, and distinctive pharmacokinetic properties with the scalability and potential cost advantages of plant molecular farming represents a largely unexplored therapeutic strategy. Accordingly,

this scoping review maps and integrates structural, biotechnological, pharmacokinetic, and clinical evidence to evaluate the feasibility of plant-produced anti-PD-L1 VHHs for NSCLC. Specifically, the review examines the molecular basis of PD-L1 recognition by VHHs, plant expression platforms and yields, the pharmacokinetic implications of VHH engineering, and the clinical efficacy and safety of PD-1/PD-L1-directed ICIs in NSCLC [46,47]. The review follows the PRISMA-ScR framework to synthesize the available evidence and identify the principal knowledge gaps requiring further preclinical and clinical investigation.

Methods

Protocol and Registration

This scoping review followed the PRISMA-ScR checklist [46,47]. The protocol was not registered prior to conducting the review. This is acknowledged as a limitation.

Eligibility Criteria

Inclusion: Original research, systematic reviews, meta-analyses, or clinical trial reports published 2012–2025 (including online-first articles with 2026 issue dates) in English, reporting on: (a) PD-L1 structure/hotspots; (b) VHH engineering/mechanisms; (c) plant expression of VHH; (d) ICI clinical outcomes in NSCLC; (e) nanobody pharmacokinetics.

Exclusion: Case reports, editorials, letters, conference abstracts; studies without quantitative data; studies on PD-L2 or CTLA-4 without PD-L1 relevance.

Information Sources and Search Strategy

PubMed/MEDLINE, Web of Science, PDB, and ClinicalTrials.gov were searched on 15 January 2026, with coverage from 2012 to 2025. Articles published online-first in late 2025 with 2026 issue dates were also included to ensure comprehensiveness.

Search Strategy

A structured, domain-specific search strategy was developed to capture evidence across three complementary datasets: structural/biochemical studies, plant biotechnology studies, and clinical evidence in NSCLC. For the structural and biochemical dataset, PubMed was searched using combinations of controlled vocabulary and title/abstract terms for PD-L1, VHHs/nanobodies, and structural or binding-related concepts, including X-ray crystallography, molecular dynamics, epitope mapping, and binding affinity. The plant biotechnology search combined VHH/nanobody-related terms with plant expression, *Nicotiana benthamiana*, molecular farming, and agroinfiltration. The clinical search targeted PD-1/PD-L1 inhibitors and immune checkpoint inhibitors in NSCLC, incorporating terms related to network meta-analysis, immune-related adverse events, safety, and pharmacokinetics. Search strategies were adapted to the indexing and controlled-vocabulary requirements of Web of Science, the Protein Data Bank (PDB), and ClinicalTrials.gov. The searches were conducted on ۱۵ January ۲۰۲۶, and database-specific strategies were documented to ensure reproducibility and comprehensive identification of relevant evidence.

Selection of Sources of Evidence

Two reviewers independently screened records. Disagreements were resolved by consensus. Inter-rater agreement was assessed using Cohen's kappa ($\kappa = 0.82$ for title/abstract screening; $\kappa = 0.91$ for full-text review).

Data Charting

Data were extracted using a standardized form including: PDB ID, KD, KD measurement method, mechanism, plant host, expression system, yield (± SD where available), HR OS, HR PFS, irAE grade, and PK parameters.

Critical Appraisal

The methodological quality and risk of bias of the included evidence were assessed using validated, design-specific appraisal tools. Randomized controlled trials were evaluated using the Cochrane Risk of Bias 2 (RoB 2) tool [48], non-randomized studies using the Risk Of Bias In Non-randomized Studies of Interventions (ROBINS-I) framework [49], and systematic reviews using the AMSTAR 2 (A MeaSurement Tool to Assess systematic Reviews 2) instrument [50]. These assessments were used to characterize the methodological limitations of the available evidence and to inform the interpretation of the findings.

Results

The evidence synthesis integrated structural, biochemical, plant-biotechnology, pharmacokinetic, and clinical data to characterize the current landscape of PD-L1-targeting VHHs. Overall, the findings support the structural and technological feasibility of VHH-based PD-L1 inhibition and plant molecular farming, while highlighting substantial gaps in target-specific production and translational validation. The results are presented across four domains: PD-L1 structure and VHH mechanisms, plant-based VHH production, clinical evidence for ICIs in NSCLC, and VHH pharmacokinetics.

Data were synthesized narratively by four axes: (A) structural mechanisms, (B) plant expression, (C) clinical efficacy/safety, (D) pharmacokinetics.

Table A: Cochrane RoB 2 assessment of randomized controlled trials

Trial	Randomization	Deviations from intended interventions	Missing outcome data	Measurement of outcome	Selection of reported result	Overall risk
KEYNOTE-024	Low	Low	Low	Low	Low	Low
KEYNOTE-042	Low	Low	Low	Low	Low	Low
KEYNOTE-189	Low	Low	Low	Low	Low	Low

KEYNOTE-407	Low	Low	Low	Low	Low	Low

Table B: ROBINS-I assessment of non-randomized studies

Study	Confounding	Selection of participants	Classification of interventions	Deviations from intended interventions	Missing data	Measurement of outcomes	Selection of reported result	Overall risk
Ge 2024 (real-world)	Moderate	Low	Low	Low	Low	Moderate	Low	Moderate

Table C: AMSTAR 2 Assessment of Systematic Reviews and Network Meta-Analyses

Review	Protocol registered	Search strategy comprehensive	Study selection reproducible	Risk of bias assessed	Meta-analytical methods appropriate	Heterogeneity assessed	Publication bias assessed	Overall confidence
Yang 2024	Yes	Yes	Yes	Yes	Yes	Yes	Yes	High
Li 2023	Yes	Yes	Yes	Yes	Yes	Yes	Yes	High
Liu 2025	Yes	Yes	Yes	Yes	Yes	Yes	Partial	Moderate
Wenfan	Yes	Yes	Yes	Yes	Yes	Yes	Yes	High

2023								
Al-Showbaki 2025	Yes	Yes	Yes	Yes	Yes	Yes	Partial	Moderate

Study selection followed the PRISMA-ScR framework and is presented in Figure 1.

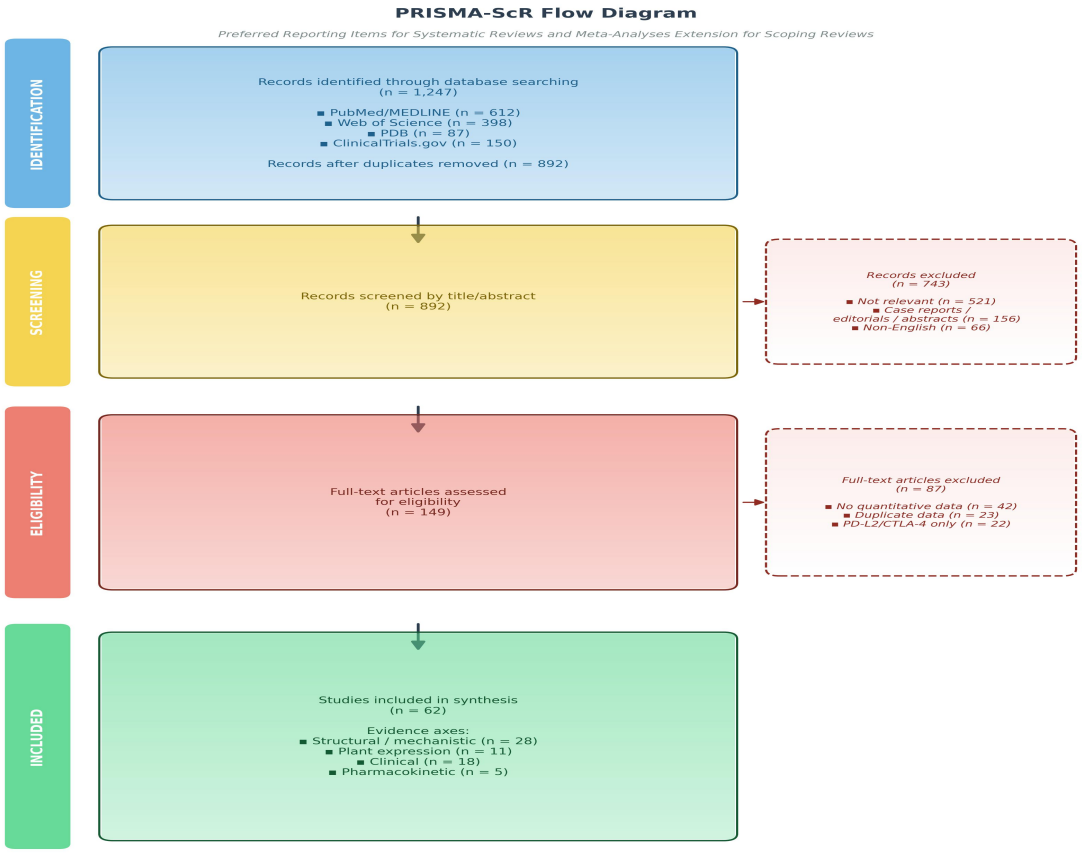

Figure 1: PRISMA-ScR flow diagram of study selection.

Records were identified from four databases (PubMed/MEDLINE, Web of Science, PDB, ClinicalTrials.gov). After removing duplicates (n = 355), 892 records were screened, 149 full-text articles assessed, and 62 studies included in the final synthesis across four evidence axes: structural/mechanistic (n = 28), plant expression (n = 11), clinical (n = 18), and pharmacokinetic (n = 5). Abbreviations: PRISMA-ScR, Preferred Reporting Items for Systematic Reviews and Meta-Analyses Extension for Scoping Reviews; PDB, Protein Data Bank.

Theoretical and Biochemical Basis of PD-L1 Inhibition

Structure of PD-L1 and Hotspots

PD-L1 (B7-H1/CD274) is a type I transmembrane glycoprotein of approximately 40 kDa [4,5]. Its extracellular region contains an IgV-like domain (PD-L1 D1) that binds PD-1 and a membrane-proximal IgC-like domain (PD-L1 D2) [6]. The IgV domain also binds the co-stimulatory receptor CD80 (B7-1) [4].

Crystallographic and cryo-EM analyses have identified key PD-L1 hotspots for PD-1 binding: F19, Y56, M115, I54, and R113 [51,52]. These residues form a steric competitive epitope targeted by therapeutic mAbs and competitive VHHs [53]. Computational analyses have further identified three main hot spots on the PD-L1 surface: the deepest cleft comprising Tyr56, Glu58, Arg113, Tyr123, and Met115; a second hot spot formed by Met115, Ala121, and Tyr123; and a third hot spot constituted by a shallow groove [51].

The KN035 nanobody competes with PD-1 for the same flat surface on PD-L1 through a single 21-amino-acid loop that forms two short helices and interacts with I54, Y56, and R113 [28]. Mutagenesis studies explain the approximately 1,000-fold stronger binding of KN035 to PD-L1 than PD-1 [28].

PD-L1 is subject to post-translational modifications, particularly glycosylation at N35, N192, N200, and N219, which stabilizes PD-L1 on the cancer cell surface and contributes to immune evasion [54,55]. Aberrant N-glycosylation at N35 can modulate the blocking capacity of ICIs [55]. VSTM2A acts as a natural PD-L1 antagonist [56], and hypoxia upregulates PD-L1 expression [57]. CD80 and PD-1 share an overlapping binding site on PD-L1, enabling dual VHH blocking [29,30].

VHH Structure and Mechanisms

VHHs are single-domain antibodies derived from camelid heavy-chain antibodies [25]. They are ~15 kDa, have high thermal stability (>70°C), and possess extended CDR3 loops that target cryptic epitopes [25,26]. VHHs lack the Fc domain, resulting in rapid renal clearance (half-life of hours) [17].

VHHs can block PD-L1/PD-1 through steric competition [28,29] or dually block PD-L1/CD80 through shared epitopes such as R113 and M115 [29]. A panel of 16 novel VHHs specific to PD-L1 has been characterized with affinities ranging from 0.7 nM to 5.1 μM [29].

Research Background

Table 1: Solved PD-L1 structures and VHH inhibition mechanisms

Row	Lead Author (Year)	PDB ID	PD-L1 Epitopes	Mechanism	KD (nM)	KD Method	Key Finding	Ref
1	Zhang (2017)	5JDS	I54, Y56, R113	Steric competitive	~0.5	SPR	KN035 nanobody; 21-aa loop	[28]
2	Kang-	7ZH4	R113,	Dual (PD-1/CD80)	0.38	BLI	B7 pathway	[29]

	Pettinger (2023)		M115				inhibition	
3	Liu H (2019)	N/A	Y56 axis	Low-MW peptide	310	SPR	Peptide stability challenge	[58]
4	Giannetti M (2025)	N/A	L122, M115	Nanostructure/MD	60	ITC	MD optimization	[59]
5	Butte (2007)	PD-L1/B7-1	IgV domain	N/A	—	—	PD-L1/CD80 interaction	[4]
6	Guo (2026)	Review	N/A	N/A	—	—	Nanobody cancer therapy	[60]

Abbreviations: PDB, Protein Data Bank; KD, dissociation constant; SPR, surface plasmon resonance; BLI, biolayer interferometry; ITC, isothermal titration calorimetry; MD, molecular dynamics; MW, molecular weight; N/A, not applicable.

Plant-Based Production of VHHs

Plant Expression Systems

Plant molecular farming offers low production costs, scalability, and freedom from human pathogens [33,34]. Transient agroinfiltration in N. benthamiana is the most widely used platform, with production timelines of days to weeks [36,61].

Expression Strategies and Yields

Table 2: Plant expression systems for VHH production

Expression System	Host	Reported Yield	Advantages	Limitations	Ref
Transient agroinfiltration	N. benthamiana	up to 110.90 ± 6.46 mg/kg FW (VHH-Fc, chloroplast-	Rapid, scalable	Labor-intensive	[43]

		targeted)			
Stable transformation	A. thaliana	seeds ~0.2 mg/g FW (VHH-Fc)	Convenient storage	Lower yield	[41]
Transplastomic	Tobacco chloroplast	2–5% TSP	Very high yield	Non-glycosylated proteins only	[62,63]

Abbreviations: VHH, variable heavy chain domain of heavy-chain antibodies; VHH-Fc, VHH fused to Fc domain; FW, fresh weight; TSP, total soluble protein.

Note: Yield values are for VHH or VHH-Fc fusions expressed in plants, not for PD-L1-specific VHHs. The 110.90 ± 6.46 mg/kg FW value derives from a chloroplast-targeted VHH-Fc fusion against enterohemorrhagic E. coli O157:H7 [43], and is therefore not PD-L1-specific. Subcellular targeting (apoplast, ER, chloroplast) significantly affects yield [41,43].

Plant-Produced Anti-PD-L1 Antibodies

Plant-produced atezolizumab and pembrolizumab demonstrate PD-L1 binding equivalent to mammalian cell-produced counterparts [42]. However, these are full-length mAbs (~150 kDa) and do not address the PK limitations of mAbs.

Biosafety and Regulatory Considerations

The regulatory landscape for plant-made pharmaceuticals is complex. In the USA, the FDA oversees plant-derived recombinant pharmaceuticals through its Centre for Biologics Evaluation and Research (CBER) and Centre for Drug Evaluation and Research (CDER), and the transition from preclinical to clinical development requires an investigational new drug (IND) application [64]. In the EU, genetically modified organism (GMO) regulation is established through Directive 2001/18/EC on deliberate release and Directive 2009/41/EC on contained use [65]. Field production of pharmaceutical crops requires permits and containment plans, and EU regulations permit a tolerance threshold of up to 0.5% for adventitious GM presence in non-GM crops where unavoidable [65]. A unified global regulatory standard for plant-made pharmaceuticals does not yet exist, though recent reviews highlight progress in closed-loop systems that maintain identity preservation and containment throughout the product lifecycle [66].

The findings of this study are organized around three major domains: the structural basis of PD-L1 inhibition by VHH nanobodies, the production of VHHs in plant-based expression systems, and the pharmacokinetic comparison of different antibody formats. Figure 2 illustrates the structural basis of PD-L1 recognition and inhibition by VHHs, highlighting key binding hotspots, steric competition with PD-1, and the molecular interactions between the KN035 nanobody and PD-L1. Figure 3 presents the major steps involved in VHH production in *Nicotiana benthamiana*, from construct design and *Agrobacterium*-mediated agroinfiltration to protein extraction, purification, and quantitative and qualitative assessment. Figure 4 compares mAbs, VHH-Fc, and unengineered VHHs in terms of molecular weight, plasma half-life, tumor penetration, and other

properties relevant to therapeutic application. Collectively, these figures illustrate the relationship between the structural characteristics of VHHs, their feasibility for production in plant-based systems, and the potential pharmacokinetic implications of different antibody formats for PD-L1 targeting.

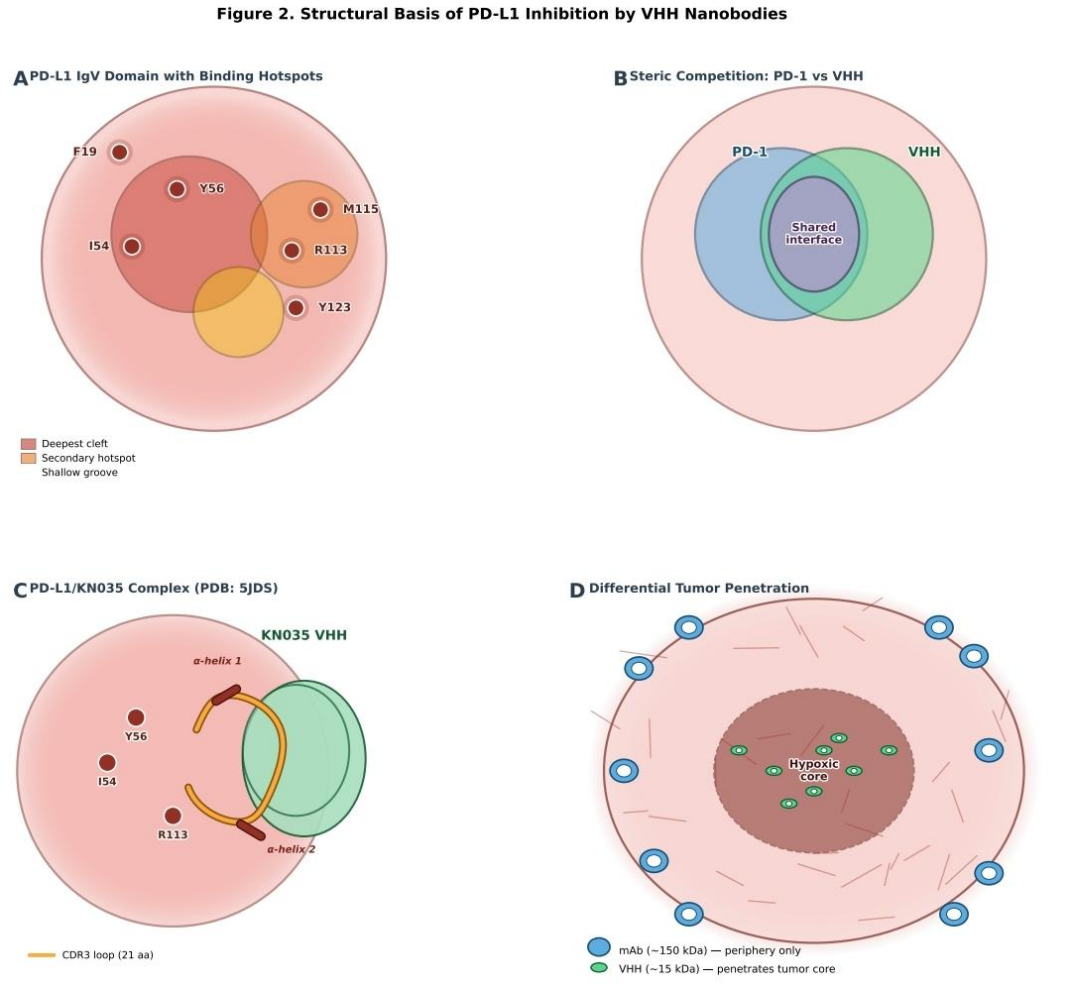

Figure 2: Structural basis of PD-L1 inhibition by VHH nanobodies

(A) Surface representation of the PD-L1 IgV domain with key hotspots labeled: F19, I54, Y56, R113, M115, Y123. Colors indicate binding pockets (dark red = deepest cleft; orange = secondary hotspot; yellow = shallow groove). (B) Overlay of PD-1 and VHH binding sites on PD-L1, illustrating steric competition for the shared interface. (C) Crystal structure of PD-L1 in complex with KN035 nanobody (PDB: 5JDS), showing the 21-amino-acid CDR3 loop and its hydrophobic/ionic interactions with I54, Y56, and R113. (D) Size comparison of mAb (~150 kDa) vs VHH (~15 kDa) relative to tumor extracellular matrix. Abbreviations: PD-L1, programmed death-ligand 1; PD-1, programmed cell death protein 1; VHH, variable heavy chain domain of heavy-chain antibodies; mAb, monoclonal antibody; CDR, complementarity-determining region.

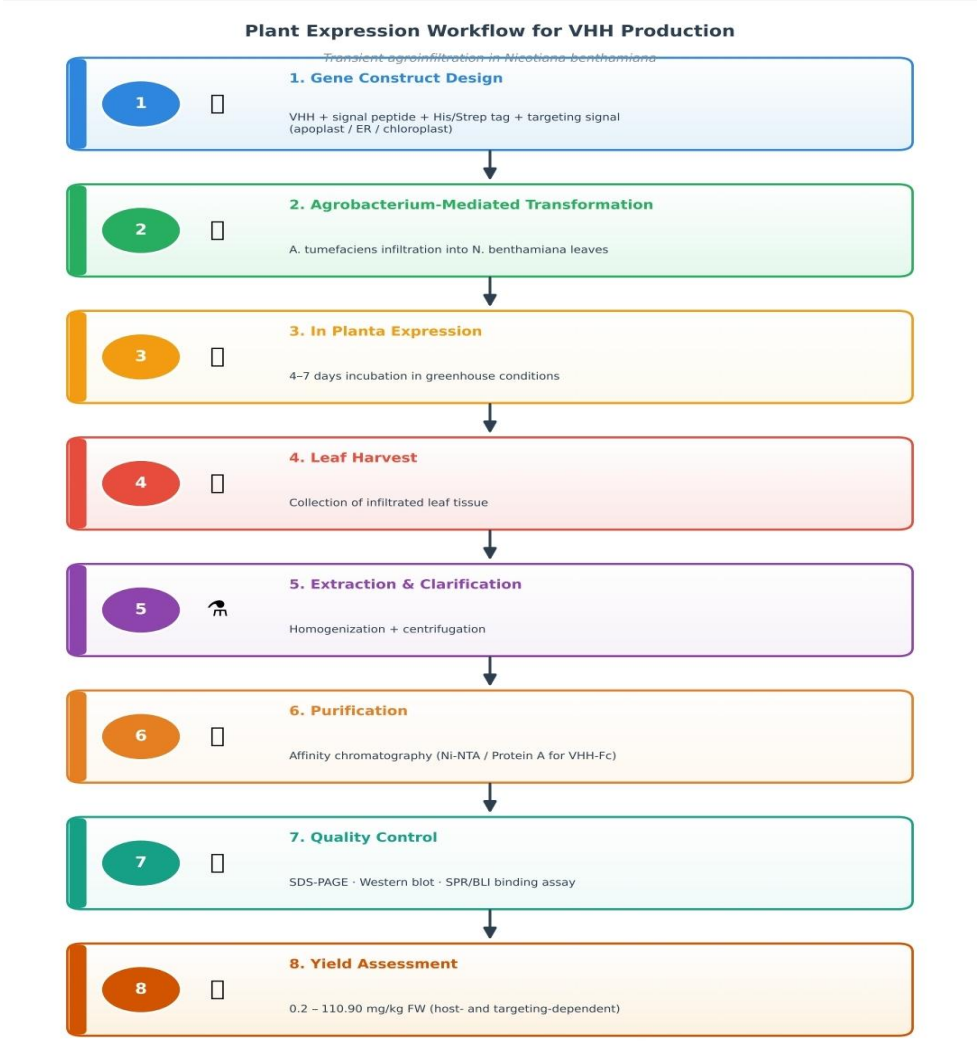

Figure 3: Plant expression workflow for VHH production

Schematic representation of the transient agroinfiltration pipeline in Nicotiana benthamiana: (1) gene construct design with signal peptide, purification tag, and subcellular targeting signal; (2) Agrobacterium tumefaciens-mediated transient transformation; (3) in planta expression (4–7 days); (4) leaf harvest; (5) extraction and clarification; (6) affinity chromatography purification; (7) quality control (SDS-PAGE, Western blot, SPR/BLI); (8) final yield assessment (0.2–110.90 mg/kg fresh weight, depending on host and subcellular targeting). Abbreviations: VHH, variable heavy chain domain of heavy-chain antibodies; SPR, surface plasmon resonance; BLI, biolayer interferometry; FW, fresh weight.

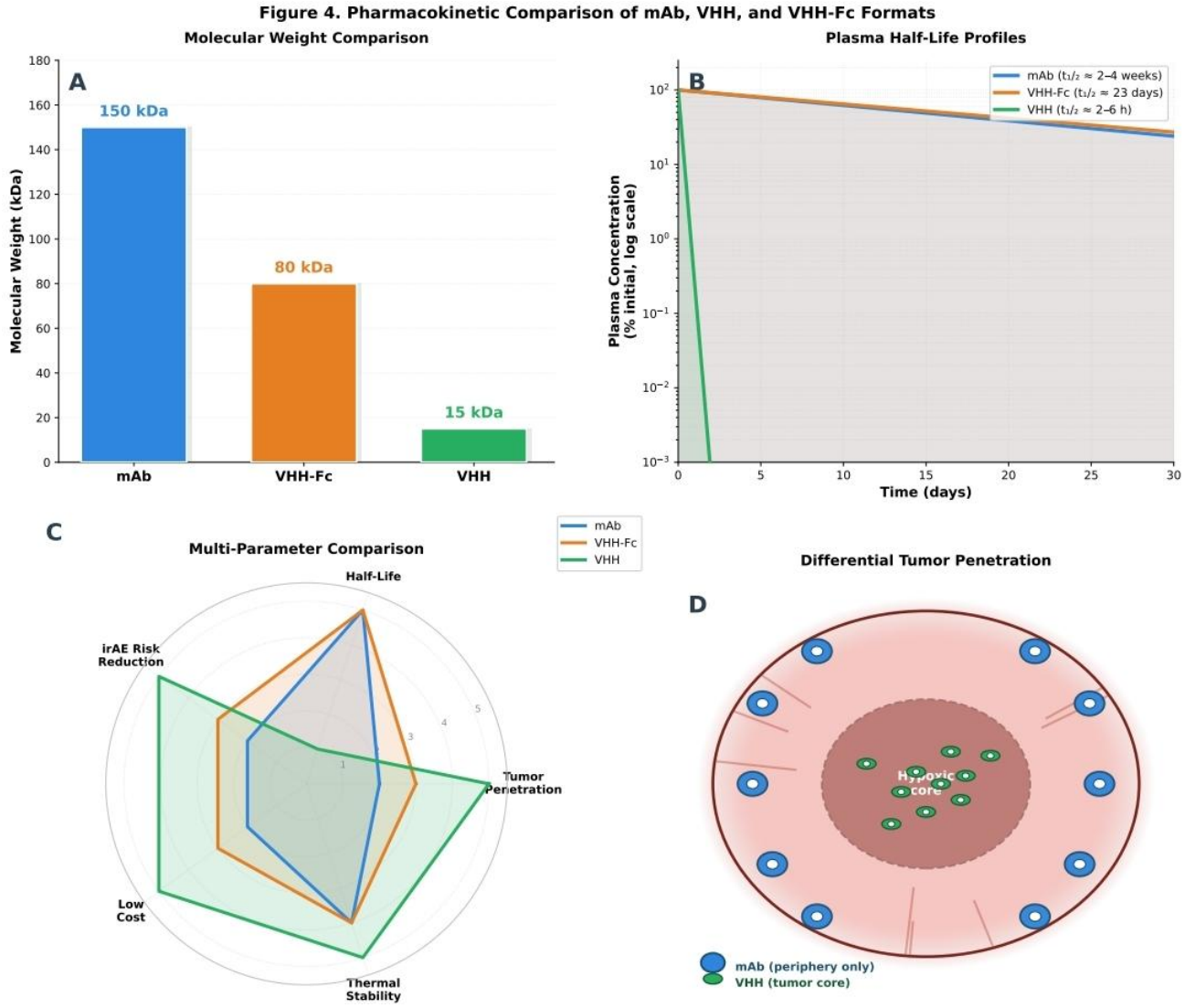

Figure 4: Pharmacokinetic comparison of mAb, VHH, and VHH-Fc formats

(A) Bar chart comparing molecular weights: mAb (150 kDa), VHH-Fc (~80 kDa), VHH (15 kDa). (B) Plasma half-life curves (log scale): mAb 2–4 weeks, VHH-Fc ~23 days, unengineered VHH 2–6 hours. (C) Radar chart comparing five parameters across the three formats: tumor penetration, half-life, irAE risk, manufacturing cost, and thermal stability. (D) Schematic illustrating differential tumor penetration: mAbs restricted to the tumor periphery vs VHHs penetrating into the tumor core. Abbreviations: mAb, monoclonal antibody; VHH, variable heavy chain domain of heavy-chain antibodies; VHH-Fc, VHH fused to Fc domain; irAE, immune-related adverse event.

Clinical Landscape of ICIs in NSCLC

Efficacy of ICI Regimens

Table 3: Efficacy of ICI regimens in NSCLC: clinical trial data

Regimen	Trial	Population	HR OS (95% CI)	HR PFS (95% CI)	Grade ≥3 immune-mediated AEs	Ref
Chemotherapy alone	—	All advanced	1.00 (Ref)	1.00 (Ref)	—	—
Pembrolizumab mono	KEYNOTE-024	PD-L1 ≥50%	0.63 (0.47–0.86)	0.50 (0.37–0.68)	7.5–8.5%	[9]
Pembrolizumab mono	KEYNOTE-042	PD-L1 ≥1%	0.81 (0.71–0.93)	1.07 (0.94–1.21)	7.5–8.5%	[10]
Pembrolizumab + chemo	KEYNOTE-189	Non-squamous	0.49 (0.38–0.64) initial; 0.56 (0.45–0.70) updated	0.52 (0.43–0.64)	7.5–8.5%	[11,13]
Pembrolizumab + chemo	KEYNOTE-407	Squamous	0.64 (0.49–0.85)	0.56 (0.45–0.70)	9.5–10.5%	[12]

Abbreviations: ICI, immune checkpoint inhibitor; NSCLC, non-small cell lung cancer; HR, hazard ratio; OS, overall survival; PFS, progression-free survival; CI, confidence interval; AEs, adverse events; mono, monotherapy; chemo, chemotherapy; Ref, reference.

Note: SCLC trials are outside the scope of this review and are therefore not included in this table.

Note: In KEYNOTE-189, immune-mediated adverse events of Grade 3–4 occurred in approximately 7.5–8.5% of patients. Rates reported for "all adverse events" (including chemotherapy-related events such as neutropenia) should not be conflated with immune-mediated adverse events, which reflect a distinct mechanistic category.

Note: Values in the "Grade ≥3 immune-mediated AEs" column reflect Grade 3–4 immune-mediated events only. When infusion-related reactions are included in the composite endpoint, rates reach approximately 10.9% in KEYNOTE-189 [13].

Structural Description of PD-L1

Table 4: Structural description of PD-L1

Row	PDB ID	Structure	Key PD-1 Residues	VHH Targeting	Ref
1	2HR1	PD-L1/PD-1	F19, Y56, M115	Competitive	[51]
2	7ZH4	PD-L1/dual VHH	R113, M115	Dual (Kang-Pettinger)	[29]
3	3SB0	PD-L1 alone	Flexible IgV	Rational engineering	[53]
4	5JDS	PD-L1/KN035	I54, Y56, R113	Competitive (KN035)	[28]

Abbreviations: PDB, Protein Data Bank; PD-L1, programmed death-ligand 1; PR-1, programmed cell death protein 1; VHH, variable heavy chain domain of heavy-chain antibodies; IgV, immunoglobulin variable domain.

Pharmacokinetics

Table 5: Pharmacokinetic comparison of mAbs, VHH, and VHH-Fc

Parameter	mAbs	VHH (unengineered)	VHH-Fc (e.g., envafolimab)
Molecular weight	150 kDa	15 kDa	~80 kDa
Half-life ($t_{1/2}$)	2–4 weeks	2–6 hours	~23 days
Clearance	FcRn-mediated	Rapid renal	FcRn-mediated
Tumor penetration	Poor	Excellent	Moderate

Abbreviations: mAbs, monoclonal antibodies; VHH, variable heavy chain domain of heavy-chain antibodies; VHH-Fc, VHH fused to Fc domain; FcRn, neonatal Fc receptor; $t_1/_2$, half-life.

Note: Envafolimab is a VHH-Fc fusion, not a native VHH. Its PK properties differ substantially from unengineered VHHs.

PD-L1 Regulatory Factors

Table 6: PD-L1 regulatory factors relevant to VHH design

Factor	Effect on PD-L1	Relevance to VHH
Glycosylation (N35, N192, N200, N219)	Stabilizes PD-L1	VHHs can target protected epitopes
Hypoxia	Upregulates PD-L1	Deep VHH penetration into hypoxic areas

Abbreviations: PD-L1, programmed death-ligand 1; VHH, variable heavy chain domain of heavy-chain antibodies.

Discussion

This scoping review maps evidence on plant-produced VHHs targeting PD-L1. The structural and pharmacological rationale is strong: VHHs are small (~15 kDa), stable (>70°C), and can achieve sub-nanomolar affinity [25–29]. Plant expression systems can produce VHH-Fc fusions at yields up to 110.90 ± 6.46 mg/kg FW in chloroplast-targeted constructs [43]. However, three critical gaps remain.

First, no plant-produced anti-PD-L1 VHH has been reported. The claim that plant-produced VHHs are an "alternative to mAbs" is therefore a hypothesis, not a finding. Plant-produced anti-PD-L1 mAbs exist [42], but these are full-length antibodies and do not address PK limitations.

Second, no clinical trial data exist for VHHs in NSCLC. All efficacy and safety predictions are based on PK modeling and structural studies. The relationship between half-life and irAE risk is complex and involves target expression in normal tissues, patient genetics, and immune activation pathways [19,20].

Third, yield data are inconsistent and platform-dependent. The reported yield of 110.90 ± 6.46 mg/kg FW for VHH-Fc in chloroplast-targeted N. benthamiana reflects optimized subcellular targeting and engineered disulfide bond stabilization, but this value was obtained with a non-PD-L1 target [43].

The structural data on PD-L1/VHH interactions are robust. The KN035 nanobody (PDB: 5JDS) competes with PD-1 for the same flat surface on PD-L1 through a single 21-amino-acid loop that forms two short helices and develops key hydrophobic and ionic interactions with PD-L1 residues such as Ile54, Tyr56, and Arg113 [28]. Mutagenesis studies identified hotspot residues on the PD-L1 surface and explained the approximately 1,000-fold stronger binding of KN035 to PD-L1 than PD-1 and its lack of binding to PD-L2 [28]. Computational analyses have further identified three main hot spots on the PD-L1 surface: the deepest cleft comprising

Tyr56, Glu58, Arg113, Tyr123, and Met115; a second hot spot formed by Met115, Ala121, and Tyr123; and a third hot spot constituted by a shallow groove [51].

However, the structural analysis has limitations. The KD values reported in Table 1 were measured using different methods (SPR, BLI, ITC), which can yield different absolute values. Standardization of KD measurement across studies would strengthen cross-study comparisons.

Plant molecular farming offers several theoretical advantages for VHH production. The establishment of a molecular farming facility generally requires 50–80% less capital investment than a mammalian cell culture plant, and per-unit production costs can be as low as 1–10% of conventional systems [35]. Plants are free from human pathogens, and N. benthamiana can complete a growth cycle in 4–5 weeks with transient expression enabling protein production in days to weeks [36].

The regulatory landscape for plant-made pharmaceuticals remains complex. In the USA, the FDA oversees plant-derived recombinant pharmaceuticals through CBER and CDER, and the transition from preclinical to clinical development requires an IND application [64]. In the EU, GMO regulation is established through Directive 2001/18/EC and Directive 2009/41/EC [65]. Field production of pharmaceutical crops requires permits and containment plans. A unified global regulatory standard for plant-made pharmaceuticals does not yet exist [65]. Recent frameworks for closed-loop systems that maintain identity preservation and containment are increasingly recognized as essential [66].

The clinical data for ICIs in NSCLC are robust, with multiple large randomized controlled trials demonstrating survival benefits. KEYNOTE-024 established pembrolizumab monotherapy as standard of care for PD-L1 TPS ≥50% (HR OS 0.63, 95% CI 0.47–0.86) [9]. KEYNOTE-189 demonstrated that adding pembrolizumab to chemotherapy improved OS in non-squamous NSCLC (HR OS 0.49, 95% CI 0.38–0.64 in the initial analysis; HR OS 0.56, 95% CI 0.45–0.70 in updated analysis) [11,13]. The updated analysis confirmed that the benefit was observed in patients with both PD-L1-positive and PD-L1-negative disease, as well as in patients with liver/brain metastases [13].

The irAE data require careful interpretation. In KEYNOTE-189, immune-mediated AEs and infusion-related reactions (any grade) occurred in 26.4% of patients in the pembrolizumab-combination group, with Grade 3–5 events in 10.9% [13]. This is substantially lower than the 45% figure sometimes reported for ICI combination regimens. The 45% figure represents all adverse events (including chemotherapy-related events such as neutropenia) and does not reflect immune-mediated adverse events specifically.

Limitations

This review has several limitations. First, no clinical trial data are currently available for VHHs in NSCLC, and therefore their potential efficacy and safety remain largely inferential, based on pharmacokinetic models, structural studies, and preclinical evidence. Second, no plant-produced anti-PD-L1 VHH has yet been experimentally reported, leaving the central translational hypothesis of this review untested. Third, as a scoping review, no protocol was prospectively registered, which may limit methodological transparency. The included evidence was also highly heterogeneous, encompassing structural biology, plant biotechnology, preclinical pharmacology, pharmacokinetics, and clinical trials with substantially different study designs, endpoints, and levels of evidence. In addition, some proposed mechanisms, including dual blockade of PD-1 and CD80, remain dependent on limited primary evidence and require further experimental validation. The restriction to English-language publications may have introduced language bias, while unpublished studies and negative findings may have been underrepresented because of potential publication bias. Finally, reported KD values were obtained using different analytical platforms, including surface plasmon resonance

(SPR), biolayer interferometry (BLI), and isothermal titration calorimetry (ITC), which limits direct quantitative comparison across studies.

Future Directions

Future research should prioritize proof-of-concept expression of anti-PD-L1 VHHs in *Nicotiana benthamiana*, with systematic optimization of subcellular targeting, disulfide-bond engineering, affinity, stability, and molecular half-life while preserving tumor penetration. Subsequent studies should directly compare unengineered VHHs, VHH-Fc fusions, and albumin-fused VHHs produced in plant and mammalian expression systems using standardized pharmacokinetic and pharmacodynamic endpoints. Preclinical validation should be followed by Phase I/II clinical trials in NSCLC to establish safety, tolerability, pharmacokinetics, target engagement, and preliminary efficacy, supported by biomarker-driven approaches to identify patient populations most likely to benefit. Combination strategies with chemotherapy, anti-angiogenic agents, and other immune checkpoint inhibitors should also be investigated. Dedicated structural and functional studies are needed to clarify allosteric and non-canonical mechanisms of PD-L1 inhibition, including the proposed dual PD-1/CD80 blockade. Parallel efforts should focus on scale-up, process standardization, regulatory development, and cost-effectiveness analyses of plant-based VHH manufacturing compared with conventional mammalian-cell platforms. Finally, standardization of KD measurement methods and reporting criteria across studies will be essential to enable reliable comparison of VHH binding affinities and facilitate translational development.

Conclusions

Plant-produced VHHs represent a promising but currently unproven approach for PD-L1 inhibition. The structural rationale is strong, and plant expression systems are technically feasible. However, the absence of both plant-produced anti-PD-L1 VHHs and clinical trial data means that claims of superiority over mAbs are premature. The structural data demonstrate that VHHs can achieve sub-nanomolar affinity and block PD-L1/PD-1 through steric competition or dual PD-1/CD80 blockade. The pharmacological rationale is supported by the small size (~15 kDa) of VHHs, which enables superior tumor penetration, and the lack of an Fc domain, which results in rapid renal clearance and reduced systemic exposure. The biotechnological rationale is supported by the successful expression of VHH-Fc fusions in N. benthamiana, with yields up to 110.90 ± 6.46 mg/kg FW in chloroplast-targeted constructs. However, significant gaps remain. No plant-produced anti-PD-L1 VHH has been reported. No clinical trial data exist for VHHs in NSCLC. The regulatory pathway for plant-made pharmaceuticals remains complex and lacks a unified global standard. Phase I/II trials and proof-of-concept plant expression studies are warranted to validate the structural, pharmacological, and biotechnological rationale.

Declarations

Conflict of Interest

The authors declare no competing interests.

Funding

No specific grant from any funding agency.

Author Contributions

M.B.1 (Maryam Behyari) conceived the study, performed the literature search, analyzed data, and drafted the manuscript. M.B.2 (Mahla Behyari) contributed to data interpretation and critically revised the manuscript. Both authors approved the final version.

Ethics Approval

Not applicable.

Data Availability

All data are from published sources.

AI Use Declaration

The authors used AI-assisted tools (including large language models) for language editing and reference formatting. All scientific content, analysis, and conclusions were independently verified by the authors. No references were generated by AI; all sources were manually verified against PubMed, Crossref, or DOI.org.

References

1. Topalian SL, Hodi FS, Brahmer JR, et al. Safety and activity of anti-PD-1 antibody in patients with advanced cancer. N Engl J Med. 2012;366(26):2455–65. doi:10.1056/NEJMoa1200694.
2. Sharpe AH, Pauken KE. The diverse functions of the PD1 inhibitory pathway. Nat Rev Immunol. 2018;18(3):153–67. doi:10.1038/nri.2017.108.
3. Wherry EJ, Kurachi M. Molecular and cellular insights into T cell exhaustion. Nat Rev Immunol. 2015;15(8):486–99. doi:10.1038/nri3862.
4. Butte MJ, Keir ME, Phamduy TB, Sharpe AH, Freeman GJ. Programmed death-1 ligand 1 interacts specifically with the B7-1 costimulatory molecule to inhibit T cell responses. Immunity. 2007;27(1):111–22. doi:10.1016/j.immuni.2007.05.016.
5. Dong H, Strome SE, Salomao DR, et al. Tumor-associated B7-H1 promotes T-cell apoptosis: a potential mechanism of immune evasion. Nat Med. 2002;8(8):793–800. doi:10.1038/nm730.
6. Kang-Pettinger T, Walker K, Brown R, Cowan R, Wright H, Baravalle R, Waters LC, Muskett FW, Bowler MW, Sawmynaden K, Coombs PJ, Carr MD, Hall G. Identification, binding, and structural characterization of single domain anti-PD-L1 antibodies inhibitory of immune regulatory proteins PD-1 and CD80. J Biol Chem. 2023 Jan;299(1):102769. doi: 10.1016/j.jbc.2022.102769. Epub 2022 Dec 5. PMID: 36470427; PMCID: PMC9811221.
7. Ribas A, Wolchok JD. Cancer immunotherapy using checkpoint blockade. Science. 2018;359(6382):1350–5. doi:10.1126/science.aar4060.
8. Bray F, Laversanne M, Sung H, et al. Global cancer statistics 2022: GLOBOCAN estimates of incidence and mortality worldwide for 36 cancers in 185 countries. CA Cancer J Clin. 2024;74(3):229–63. doi:10.3322/caac.21834.
9. Reck M, Rodríguez-Abreu D, Robinson AG, et al. Pembrolizumab versus chemotherapy for PD-L1-positive NSCLC. N Engl J Med. 2016;375(19):1823–33. doi:10.1056/NEJMoa1606774.
10. Mok TSK, Wu YL, Kudaba I, et al. Pembrolizumab versus chemotherapy for PD-L1-expressing NSCLC (KEYNOTE-042). Lancet. 2019;393(10183):1819–30. doi:10.1016/S0140-6736(18)32409-7.
11. Gandhi L, Rodríguez-Abreu D, Gadgeel S, et al. Pembrolizumab plus chemotherapy in metastatic NSCLC. N Engl J Med. 2018;378(22):2078–92. doi:10.1056/NEJMoa1801005.
12. Paz-Ares L, Luft A, Vicente D, et al. Pembrolizumab plus chemotherapy for squamous NSCLC. N Engl J Med. 2018;379(21):2040–51. doi:10.1056/NEJMoa1810865.
13. Gandhi L, Rodríguez-Abreu D, Gadgeel S, et al. Updated analysis from KEYNOTE-189: pembrolizumab or placebo plus pemetrexed and platinum for previously untreated metastatic nonsquamous NSCLC. J Clin Oncol. 2020;38(14):1505–17. doi:10.1200/JCO.19.03136.

14. Yang Y, Chen W, Dong L, Duan L, Gao P. Comparison of efficacy and safety of PD-1/PD-L1 combination therapy in first-line treatment of advanced NSCLC. Clin Transl Oncol. 2024;26(10):2488–502. doi:10.1007/s12094-024-03442-3.
15. Li Y, Liang X, Li H, Chen X. Efficacy and safety of immune checkpoint inhibitors for advanced NSCLC. Chin Med J (Engl). 2023;136(18):2156–65. doi:10.1097/CM9.0000000000002750.
16. Liu L, Yan Y, Wang Y, et al. Comparative efficacy and safety of first-line PD-1/PD-L1 inhibitors in NSCLC. Oncol Lett. 2025;29(3):157. doi:10.3892/ol.2025.14903.
17. Rhodes SJ, Adams GP. Immunoconjugates for cancer therapy. Mol Pharm. 2017;14(5):1239–51. doi:10.1021/acs.molpharmaceut.6b01036.
18. Kim JM, Chen DS. Immune escape to PD-L1/PD-1 blockade: seven steps to success (or failure). Ann Oncol. 2016;27(8):1492–504. doi:10.1093/annonc/mdw217.
19. Xiao J, Xia Z, Wu Z, Fang M. Clinical features, treatment, and outcomes of anti-PD-L1 induced psoriasis. Invest New Drugs. 2025;43(3):719–27. doi:10.1007/s10637-025-01554-3.
20. Xiao J, Tang S, Xia Z, Zhou Y, Fang M. Clinical presentation of PD-1/PD-L1 immune checkpoint inhibitors induced cystitis. Invest New Drugs. 2025;43(4):770–9. doi:10.1007/s10637-025-01563-2.
21. Al-Showbaki L, Al-Kasasbeh M, Jbarah K, et al. Anti-PD-1 versus anti-PD-L1 in PD-L1-negative advanced NSCLC. World J Oncol. 2025;16(3):299–310. doi:10.14740/wjon2520.
22. Liang J, Li M, Sui Q, et al. Compare the efficacy and safety of PD-1 and PD-L1 inhibitors for advanced NSCLC. Transl Lung Cancer Res. 2020;9(4):1302–23. doi:10.21037/tlcr-20-192.
23. Li ZQ, Yan HC, Gu JJ, et al. Comparative efficacy and safety of PD-1/PD-L1 inhibitors versus platinum-based chemotherapy. Pharmacol Res. 2020;160:105194. doi:10.1016/j.phrs.2020.105194.
24. Nandi S, Kwong AT, Holtz BR, et al. Techno-economic analysis of a transient plant-based platform for monoclonal antibody production. MAbs. 2016;8(8):1456–66. doi:10.1080/19420862.2016.1227901.
25. Muyldermans S. Nanobodies: natural single-domain antibodies from camelids. Annu Rev Biochem. 2013;82:775–97. doi:10.1146/annurev-biochem-063011-092449.
26. De Meyer T, Muyldermans S, Depicker A. Nanobody-based products as research and diagnostic tools. Trends Biotechnol. 2014;32(5):263–70. doi:10.1016/j.tibtech.2014.03.001.
27. Debie P, Lafont C, Defrise M, et al. Size and affinity kinetics of nanobodies influence targeting and penetration of solid tumours. J Control Release. 2020;317:34–42. doi:10.1016/j.jconrel.2019.11.014.
28. Zhang F, Wei H, Wang X, et al. Structural basis of a novel PD-L1 nanobody for immune checkpoint blockade. Cell Discov. 2017;3:17004. doi:10.1038/celldisc.2017.4.
29. Kang-Pettinger T, Walker K, Brown R, et al. Identification, binding, and structural characterization of single domain anti-PD-L1 antibodies. J Biol Chem. 2023;299(1):102769. doi:10.1016/j.jbc.2022.102769.
30. Zhao Y, Lee CK, Lin CH, et al. PD-L1:CD80 cis-heterodimer triggers the co-stimulatory receptor CD28. Immunity. 2019;51(6):1059–73. doi:10.1016/j.immuni.2019.11.003.
31. 31. Kontermann RE. Strategies for extended serum half-life of protein therapeutics. Curr Opin Biotechnol. 2011;22(6):868–76. doi:10.1016/j.copbio.2011.06.012.
32. Zvonova EA, Ershov AV, Ershova OA, et al. PASylation technology for extending the half-life of therapeutic proteins. Biotechnol Appl Biochem. 2017;64(6):802–10. doi:10.1002/bab.1571.
33. Fischer R, Buyel JF. Molecular farming – The production of recombinant proteins in plants. Curr Opin Biotechnol. 2020;61:1–8. doi:10.1016/j.copbio.2019.09.001.
34. Schillberg S, Raven N, Spiegel H, Rasche S, Buntru M. Critical analysis of the commercial potential of plants for the production of recombinant proteins. Front Plant Sci. 2019;10:720. doi:10.3389/fpls.2019.00720.
35. Behyari M, Behyari M. Expression of Intragenic LCAL4 Long Non-Coding RNAs as a Potential Diagnostic and Prognostic Marker in Female Breast Cancer. J Family Reprod Health. 2024 Jun;18(2):129-139. doi: 10.18502/jfrh.v18i2.15937.
36. Behyari M. Investigation of LncRNA LCAL4 as a new marker in the diagnosis of female breast cancer. In: Sixth International Conference on New Findings in Medical and Health Sciences with a Health Promotion Approach; 2023. Available from: https://civilica.com/doc/1944485
37. Stoger E, Fischer R, Moloney M, Ma JK. Plant molecular farming: opportunities and challenges. In: Plant Biotechnology. Springer; 2020. p. 1–30.
38. Sack M, Rademacher T, Spiegel H, et al. From gene to harvest: insights into upstream process development for the GMP production of a monoclonal antibody in transgenic tobacco plants. Plant Biotechnol J. 2015;13(8):1094–105. doi:10.1111/pbi.12438.
39. Takaiwa F, Wakasa Y. Seed-based expression system for molecular farming. In: Molecular Pharming: Applications, Challenges and Emerging Areas. Wiley; 2022. p. 189–210.

40. Teh AY, Maresch D, Klein K, et al. Characterization of VHH antibodies against cobra venom toxins produced in Nicotiana benthamiana. Sci Rep. 2024;14:8572. doi:10.1038/s41598-024-58945-5.
41. Vanmarsenille C, Elseviers J, Yperman K, et al. In planta expression of VHH-Fc antibodies. Plant Biotechnol J. 2020;18(6):1308–20. doi:10.1111/pbi.13293.
42. Bulaon CJI, Kim K, Ko K, et al. Plant-produced anti-PD-L1 monoclonal antibody for cancer immunotherapy. Bioengineering. 2025;12(1):7. doi:10.3390/bioengineering12010007.
43. Chin-Fatt A, Saberianfar R, Menassa R. A VHH-Fc fusion targeted to the chloroplast thylakoid lumen assembles and neutralizes enterohemorrhagic E. coli O157:H7. Front Plant Sci. 2021;12:686421. doi:10.3389/fpls.2021.686421.
44. Park C, Kim K, Kim Y, et al. Plant-derived anti-HER2 antibody suppresses trastuzumab-resistant breast cancer. ACS Nano. 2024;18(24):16126–40. doi:10.1021/acsnano.4c00360.
45. Lozano-Sanchez E, Moreno-Gonzalez MA, Merwais F, et al. Plant-produced viral nanoparticles decorated with nanobodies against HER2. Adv Healthc Mater. 2026;15(5):e202505936. doi:10.1002/adhm.202505936.
46. Tricco AC, Lillie E, Zarin W, et al. PRISMA Extension for Scoping Reviews (PRISMA-ScR). Ann Intern Med. 2018;169(7):467–73. doi:10.7326/M18-0850.
47. Peters MDJ, Marnie C, Tricco AC, et al. Updated methodological guidance for scoping reviews. JBI Evid Synth. 2020;18(10):2119–26. doi:10.11124/JBIES-20-00167.
48. Sterne JAC, Savović J, Page MJ, et al. RoB 2: a revised tool for assessing risk of bias in randomised trials. BMJ. 2019;366:l4898. doi:10.1136/bmj.l4898.
49. Sterne JA, Hernán MA, Reeves BC, et al. ROBINS-I: a tool for assessing risk of bias in non-randomised studies. BMJ. 2016;355:i4919. doi:10.1136/bmj.i4919.
50. Shea BJ, Reeves BC, Wells G, et al. AMSTAR 2: a critical appraisal tool for systematic reviews. BMJ. 2017;358:j4008. doi:10.1136/bmj.j4008.
51. Shi D, Zhou S, Liu X, et al. Understanding the structural and energetic basis of PD-1 and monoclonal antibodies bound to PD-L1. Biochim Biophys Acta Gen Subj. 2018;1862(3):576–88. doi:10.1016/j.bbagen.2017.11.022.
52. Zak KM, Grudnik P, Magiera K, et al. Structural biology of the immune checkpoint receptor PD-1 and its ligands PD-L1/PD-L2. Structure. 2017;25(8):1163–74. doi:10.1016/j.str.2017.06.011.
53. 53. Córdova-Bahena L, Velasco-Velázquez MA. Anti-PD-1 and anti-PD-L1 antibodies as immunotherapy against cancer: a structural perspective. Rev Invest Clin. 2020;73(1):8–16. doi:10.24875/RIC.20000341.
54. Li CW, Lim SO, Xia W, et al. Glycosylation and stabilization of programmed death ligand-1 suppresses T-cell activity. Nat Commun. 2016;7:12632. doi:10.1038/ncomms12632.
55. Wang Y, et al. Regulation of PD-L1 glycosylation and advances in cancer immunotherapy. Cancer Lett. 2025;612:217498. doi:10.1016/j.canlet.2025.217498.
56. Dong Y, Liu JJ, Zhou Y, et al. VSTM2A reverses immunosuppression in colorectal cancer by antagonizing the PD-L1/PD-1 interaction. Mol Ther. 2024;32(11):4045–57. doi:10.1016/j.ymthe.2024.09.023.
57. Noman MZ, Desantis G, Janji B, et al. PD-L1 is a novel direct target of HIF-1α, and its blockade under hypoxia enhanced MDSC-mediated T cell activation. J Exp Med. 2014;211(5):781–90. doi:10.1084/jem.20131916.
58. Liu H, Zhao Z, Zhang L, et al. Discovery of low-molecular weight anti-PD-L1 peptides for cancer immunotherapy. J Immunother Cancer. 2019;7(1):270. doi:10.1186/s40425-019-0705-y.
59. Giannetti M, Gobbo M, Litti L, et al. Unraveling the specific recognition between PD-L1 and engineered CLP002 functionalized gold nanostructures. Molecules. 2025;30(9):2045. doi:10.3390/molecules30092045.
60. Guo M, Liao R, Wang M, Wu L, Zhang Y. Nanobody-based targeted cancer therapy and immunotherapy. Acta Pharmacol Sin. 2026. doi:10.1038/s41401-025-01573-8.
61. Peyret H, Lomonossoff GP. Plant viral vectors for the expression of recombinant proteins. Curr Opin Biotechnol. 2022;73:186–92. doi:10.1016/j.copbio.2021.09.001.
62. Buyel JF, Twyman RM, Fischer R. Very-large-scale production of antibodies in plants. Biotechnol Adv. 2017;35(4):458–65. doi:10.1016/j.biotechadv.2017.03.011.
63. Nölke G, et al. Plant-made vaccines and therapeutics. In: Molecular Farming in Plants. Springer; 2023. p. 1–25.
64. FDA. Guidance for Industry: Drugs, Biologics, and Medical Devices Derived from Bioengineered Plants for Use in Humans and Animals – Regulatory Update. 2024.
65. Buyel JF. Plant molecular farming – Integration and exploitation of side streams to achieve sustainable biomanufacturing. Front Plant Sci. 2023;14:1105369. doi:10.3389/fpls.2023.1105369.
66. Bresnahan KA, et al. Closed-loop systems for plants expressing animal proteins. Front Plant Sci. 2025;16:1426290. doi:10.3389/fpls.2025.1426290.